Grid-Following and Grid-Forming Control in Power Electronic Based Power Systems: A Comparative Study

Gao, Xian; Zhou, Dao; Anvari-Moghaddam, Amjad; Blaabjerg, Frede

Published in:
IECON 2021 – 47th Annual Conference of the IEEE Industrial Electronics Society

DOI (link to publication from Publisher):
10.1109/IECON48115.2021.9589432

Publication date:
2021

Document Version
Accepted author manuscript, peer reviewed version

Grid-Following and Grid-Forming Control in Power Electronic Based Power Systems: A Comparative Study

Xian Gao, Dao Zhou, Amjad Anvari-Moghaddam, and Frede Blaabjerg

AAU Energy
Aalborg University
Aalborg, DK-9220, Denmark
xiga@energy.aau.dk, zda@energy.aau.dk, aam@energy.aau.dk, fbl@energy.aau.dk

***Abstract* - The stability of frequency is at risk with increasing penetration of power electronic converters. In this case, the power grid will lack the moment of inertia to maintain a stable voltage and frequency in the event of a large disturbance. In order to improve the stability of the power grid, traditional grid-following control is needed to be transformed to grid-forming control. This paper analyzes the control structure of grid-following control and grid-forming control. Moreover, a case study is exemplified to compare the performance of two control strategies responding to frequency disturbances. Finally, a simulation model of 15 kW grid-connected converter is built in Matlab/Simulink to discuss the performance of the grid-following and grid-forming converters under different working conditions.**

I. INTRODUCTION

During last decades, the energy demand has increased globally. As promising candidates, renewable energy sources (RESs) have been developed at a fast rate to cope with the potential energy crisis. Renewable energy systems will play an even more significant role in the future power production.

However, RESs are coupled to the power grid through power electronic converters, which have a fast response speed and provide almost no moment of inertia for the grid [1], [2]. Today's power grid relies on synchronous generators to produce mechanical inertia. These generators are very large and rigidly synchronized with each other, so only major disturbances can affect the grid frequency. Nevertheless, distributed RESs systems rarely have synchronous generators, and they generally adopt the grid-following (GFL) converters to connect to the grid, the target of which is to simply lock and follow the grid frequency. GFL converters typically operate at their rated power output and do not respond to the frequency deviation of the power grid [3]. With the increasing penetration of RESs systems, many large central power plants are phasing out. Eventually, the moment of inertia and damping of the entire power grid that the RESs systems are connected to is decreasing, which leads to a weaker ability of the power grid to deal with sudden frequency deviations. The feature of low-inertia system has a huge impact on the stable operation of the power grid. In order to improve the stability of distributed grid with highly-penetrated RESs systems, grid-forming (GFM) control strategies have been proposed in the literature [4]. One of popular GFM control strategies is to apply the virtual synchronous generator (VSG), in which the converters are mimicking the behavior of the conventional synchronous generators (SG) in a way to improve the system inertia and damping [5].

This paper illustrated the aforementioned issues and discussed the performance of the GFL converter and GFM converter under various operation conditions. The main contributions of this paper can be summarized as follows. 1) Typical control diagrams of both the GFL control and GFM control were illustrated in detail. 2) The comparison between the GFL converter and GFM converter were discussed under different working conditions. 3) Based on the simulation results, it is revealed that the smaller the short-circuit ratio (SCR) becomes, the larger influence the load fluctuation has on the power grid, and the GFM converter is more suitable for the weak power grid with the low inertia.

The remaining part of the paper is organized as follows. Section II describes the conceptual differences between GFL converters and GFM converters. The control diagrams of both GFL and GFM converters are illustrated in Section III and Section IV, respectively. In Section V, a simulation model is built in Matlab/Simulink to compare the different performance of GFL converters and GFM converters under various working conditions and verify the expected outcomes. Finally, Section VI concludes the work.

II. GRID-FOLLOWING CONVERTERS AND GRID-FORMING CONVERTERS

According to their operation and impact to the power grid, the power converters can be classified into GFL converters and GFM converters. The GFL converter behaves approximately like a controlled current source, as shown in

Fig. 1(a). It usually adopts a phase-locked loop (PLL) to track the grid phase angle to keep the converters synchronized to the power grid [6]. The measured phase angle is then used for the current control. The GFL converter achieves the objective power injection through regulating the active current and reactive current injected into the power grid. During the disturbances such as load deviations, the GFL converter just keeps the output currents constant. However, it cannot directly provide frequency and voltage regulation for the power grid, and it relies on an extra voltage source or the power grid to provide the frequency and voltage references [7]. Thus, the GFL converter is not able to operate in an islanded mode and to deal with the problem of frequency disturbances.

On the contrary, the GFM converter behaves approximately like a controlled voltage source, as shown in Fig. 1(b). Some GFM control strategies do not need a PLL to measure the grid phase angle and are able to realize the self-synchronization with the power grid through mimicking the power synchronization principles of the conventional synchronous generators [8]. Compared to the traditional synchronous generators which provide frequency stability through the stored energy in the spinning rotors, GFM converters can adjust the output faster to cope with the frequency disturbances in the power grid [9]. Due to the frequency and voltage regulation provided by the GFM converters, they are suitable for operation in islanded modes.

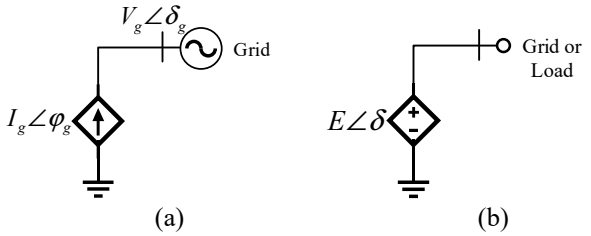

Fig. 1. Simplified representation of power converters.

(a) Grid-following converter; (b) Grid-forming converter.

In addition, some literatures illustrate that the use of a PLL with current control may reduce the stability margin of the power converters in a weak grid. That is because the GFL converter tracks the point of common coupling (PCC) voltage, which is easily affected by its output current in a low SCR grid [8]. In contrast, the GFM converter can realize the self-synchronization based on its output active power, which allows it to synchronize with a low SCR grid. However, in a stiff grid, little phase changes between the converter and grid voltages may lead to large active power fluctuations, which may induce the condition of overload [6]. The advantages and disadvantages of GFL control and GFM control are summarized in Table I.

Table I
COMPARISON OF GFL CONTROL AND GFM CONTROL.

Control mode	Advantages	Disadvantages
GFL control	1. Quick regulation [7] 2. Simple control structure [10]	1. Lack regulation of frequency and voltage [7] 2. Unable to operate in an islanded mode [6], [7] 3. Instability in weak grids [6], [8]
GFM control	1. Able to operate in an islanded mode [6], [7] 2. Provide the regulation of frequency and voltage [7]	1. Small-signal instability in stiff grids [6] 2. Easy to suffer from overload [6]

III. CONTROL STRUCTURE OF GRID-FOLLOWING CONVERTER

The GFL control is widely applied in the grid-connected converters. When the grid-connected power converters act as the interface between the power grid and the RESs, the GFL converters are mostly equipped with a PLL and a dual-loop vector control strategy. GFL converters use the PLL to track the phase angle of the PCC and adopt the vector control strategy to adjust the active current and reactive current rejected into the power grid. For this control strategy, the power grid needs to provide rigid voltage and frequency support, while the converters rarely consider voltage and frequency regulation. In this paper, the PQ control is adopted. The outer loop is dedicated to regulate the output power of the converter, while the inner current is generally to regulate the grid current according to the reference set by the outer power loop [10].

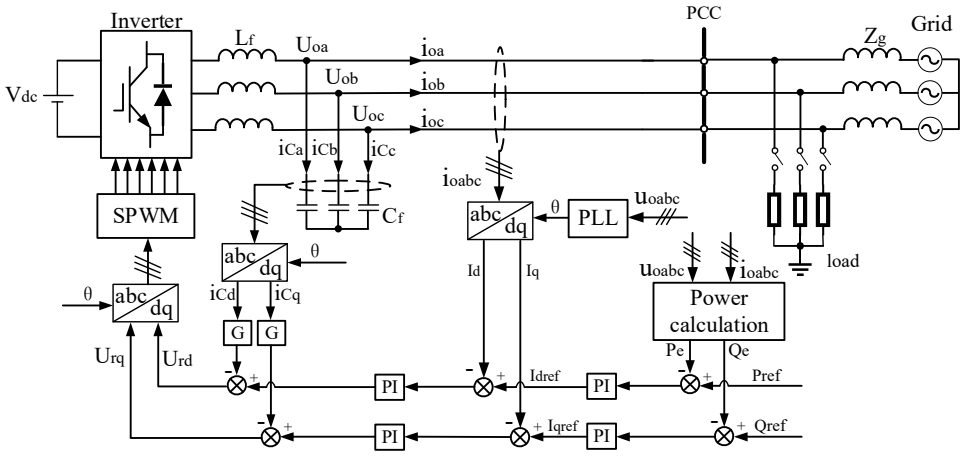

Fig. 2. PQ control structure of a grid-following converter.

The system configuration of case study with the PQ control is shown in Fig. 2, where V_{dc} is the DC bus voltage; U_{oa}, U_{ob} and U_{oc} are the output voltages of the converter; i_{oa}, i_{ob} and i_{oc} are the grid currents; i_{Ca}, i_{Cb} and i_{Cc} are the capacitor currents; L_f and C_f are the filter inductance and filter capacitance, respectively; Z_g is the impedance of the grid. In this paper, the active damping method representing a virtual resistor is adopted to avoid sacrificing the efficiency of the converter [11]. As shown in Fig. 2, the capacitor current is feedbacked in the control loop to emulate the presence of a real resistor.

IV. Control Structure of Grid-Forming Converter

With the increasing penetration of distributed RESs, the moment of inertia and damping of the entire power grid is decreasing, which may pose a great challenge to the stability of the power grid. In addition, the power of the RESs injecting into distribution lines depends on environmental conditions, being of high randomness and volatility, which aggravates the instability of power grid. Recently, as one of GFM control strategies, the VSG control technology has attracted increasing attentions because it enables the converters to mimic the inertia and damping characteristics of synchronous generators. Therefore, the power grid will have a strong ability to cope with the fluctuations of RESs and loads. Since the control strategy mainly depends on grid-connected converter, the energy management of the DC side is not considered in this work. In order to simplify the analysis, the DC side is equivalent to a DC source. The case study system with the VSG control is shown in Fig. 3, where P_e and Q_e are the output active power and reactive power; P_{ref} and Q_{ref} are the active power and reactive power references; E_m and θ are the amplitude and phase angle of reference voltage, respectively.

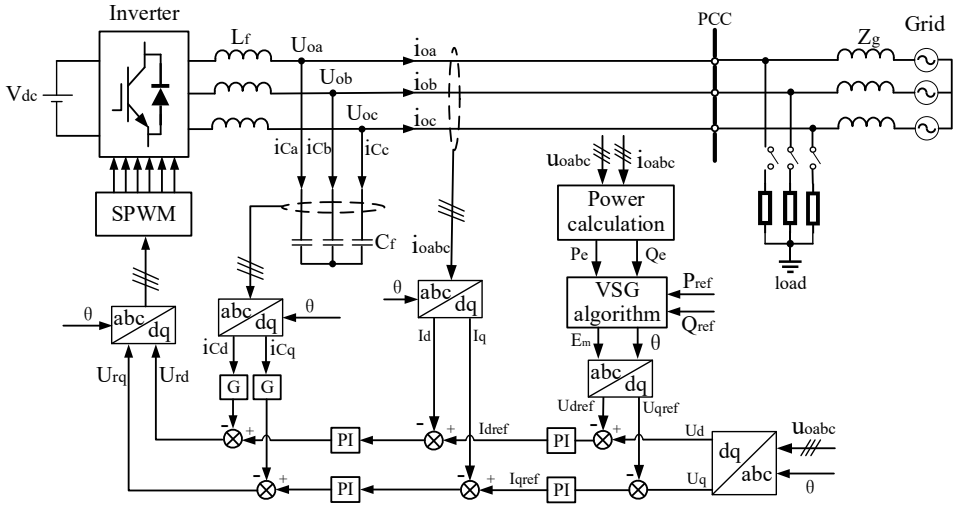

Fig. 3. VSG control structure of a grid-forming converter.

It is well known that the VSG algorithm mainly consists of power-frequency controller and excitation controller. Power-frequency controller emulates the rotor motion equation, which is also called the swing equation. Excitation controller adopts proportional component to realize the control of voltages. The swing equation and the E_m can be given as [12], [13]:

$$\begin{cases} J\dfrac{d\omega}{dt} = \dfrac{P_{ref}}{\omega} - \dfrac{P_e}{\omega} - D(\omega - \omega_0) \\ \dfrac{d\theta}{dt} = \omega \end{cases} \tag{1}$$

$$k_q \frac{dE_m}{dt} = Q_{ref} - Q_e + K_u (U_N - U_o) \tag{2}$$

where J is the moment of inertia; D is the damping coefficient; ω_0 is the rated frequency; E_0 is the rated voltage; K_q is the integrity coefficient; K_u is the voltage droop coefficient. According to the above formulas, the control diagram of the VSG algorithm is shown in Fig. 4.

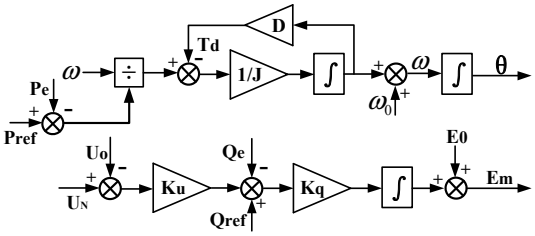

Fig. 4. Control diagram of the VSG algorithm.

V. Simulation Results

A simulation model of 15 kW grid-connected converter is established in Matlab/Simulink to demonstrate the aforementioned control schemes. The key parameters of the case study system are listed in Table II [14].

A stiff power grid with SCR=7.5 is chosen to compare the performance of GFL and GFM control. The loss of generation and the sudden load shed are selected to compare the dynamic responses of the GFL converter and the GFM converter. In addition, in order to discuss the different performance of the GFL converter and the GFM converter in a weak power grid, a

simulation under different SCR is carried out under the condition of the sudden load increase.

According to the abnormal operating performance category III in IEEE 1547-2018 standard [15], the normal operating range of the system frequency is from 58.8 Hz to 62.0 Hz and the rated frequency is 60.0 Hz. The maximum of the frequency drop is 0.02 p.u. and the maximum of frequency increase is 0.03 p.u. In addition, the rate of change of frequency (RoCoF) shall not exceed 3.0 Hz/s. As a result, the normal frequency range is from 48.3 Hz to 51.5 Hz and the RoCoF limit is 2.5 Hz/s in this case study.

Table II
PARAMETERS OF 15 KW GRID-CONNECTED CONVERTER.

Grid		
V_g	Grid voltage	220 V
f_g	Grid frequency	50 Hz
L_g	Grid impedance	4 mH
R_g	Grid resistance	0.2 Ω
Converter		
V_{dc}	DC-side voltage	700 V
L_f	Filter impedance	3 mH
C_f	Filter capacitance	20 μF
P_{set}	Rated active power	15 kW
f_s	Switching frequency	20 kHz
Controllers for grid-following converter		
(K_p, K_i, K_d)	PID controller parameters of phase-locked loop	(180, 3200, 1)
(K_{p_PQ}, K_{i_PQ})	PI controller parameters of power loop	(0.001, 0.03)
(K_{p_i}, K_{i_i})	PI controller parameters of current loop	(5, 120)
K_{p_ic}	P controller parameter of capacitor current feedback	15
Controllers for grid-forming converter		
(K_{p_v}, K_{i_v})	PI controller parameters of voltage loop	(0.1, 330)
(K_{p_i}, K_{i_i})	PI controller parameters of current loop	(5, 120)
K_{p_ic}	P controller parameter of capacitor current feedback	15
D	Damping coefficient	25
J	Virtual inertia	0.2 kg/m^2
K_u	Q-U loop coefficient	1/15
K_q	Integrity coefficient	150

A. Under a loss of generation

During 2~3s, the loss of generation happens and the active power of generation decreases from 15 kW to 10 kW.

The reference and feedback of output active power and reactive power, and the grid currents under the dq axis for the GFL converter are shown in Fig. 5. It can be seen that both outer power loop and inner current loop can well track the references during the transient.

Similarly, the reference and feedback of active power and reactive power, the output voltages and the grid currents under the dq axis for the GFM converter are shown in Fig. 6. The VSG algorithm can work well, and both the voltage loop and inner current loop can track the given references.

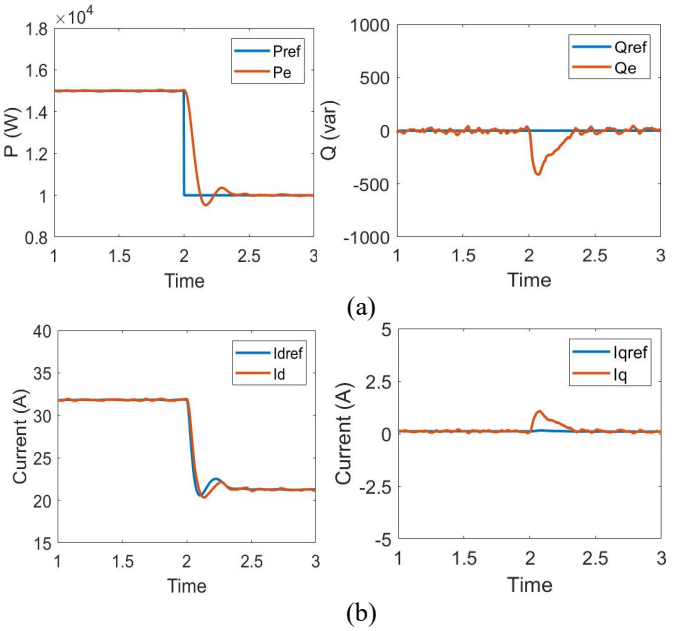

Fig. 5. Controllers of the grid-following converter. (a) Outer power loop; (b) Inner current loop.

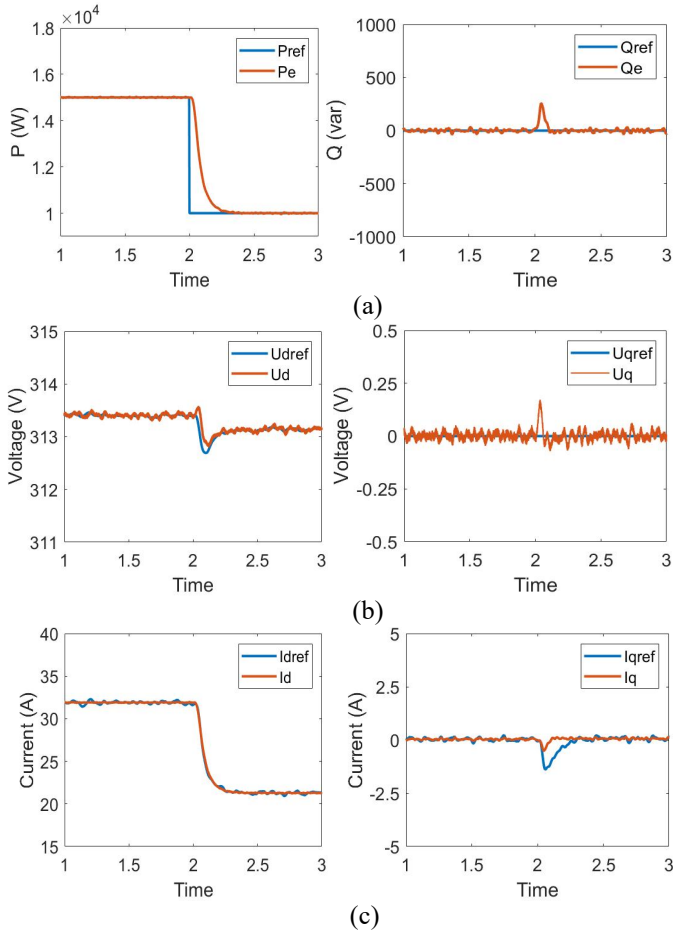

Fig. 6. Controllers of the grid-forming converter. (a) VSG algorithm; (b) Voltage loop; (c) Inner current loop.

The simulation waveforms of the converter output power, frequency, and the RoCoF at the PCC are shown in Fig. 7. It is noteworthy that the frequency and the RoCoF of the GFL converter are measured from PLL unit, while the frequency and the RoCoF of the GFM converter are measured from VSG algorithm unit. Compared to the PQ control, the VSG control slows down the change of the converter output, reflecting the inertial response characteristics. Furthermore, the VSG control provides a higher frequency nadir and a lower RoCoF, which improves the frequency stability of the power grid and have a strong ability to cope with the fluctuations of RESs.

B. *Under a sudden load shed*

During 2~3s, a sudden load shed of 10 kW is applied to the power grid. The simulation waveforms of the converter output power, frequency, and RoCoF at the PCC are shown in Fig. 8. The VSG control generates less active power to avoid the sudden increase of frequency, which improves the ability of power grid to cope with the load fluctuations. As shown in Fig. 8, the frequency culmination decreases and the RoCoF decreases through the VSG control.

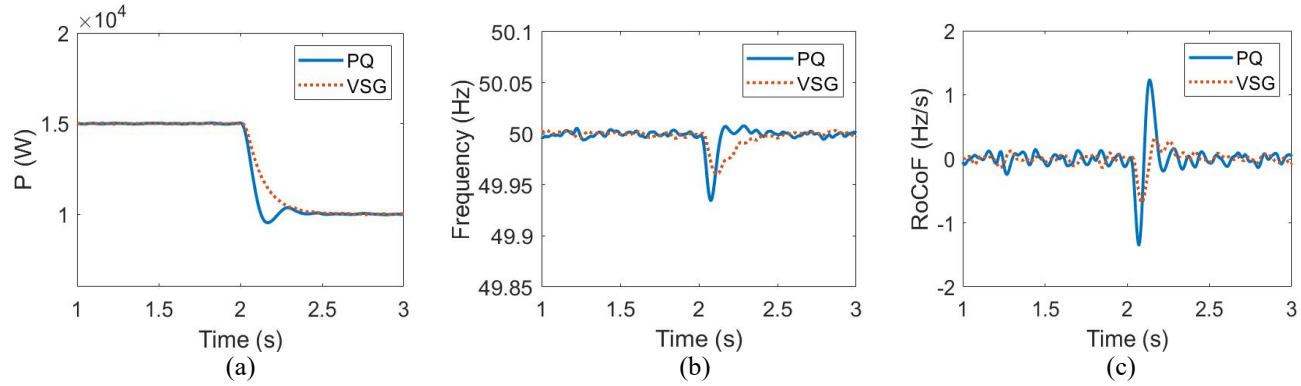

Fig. 7. Simulation waveforms under a loss of generation. (a) Inverter output power; (b) Frequency at the PCC; (c) RoCoF at the PCC.

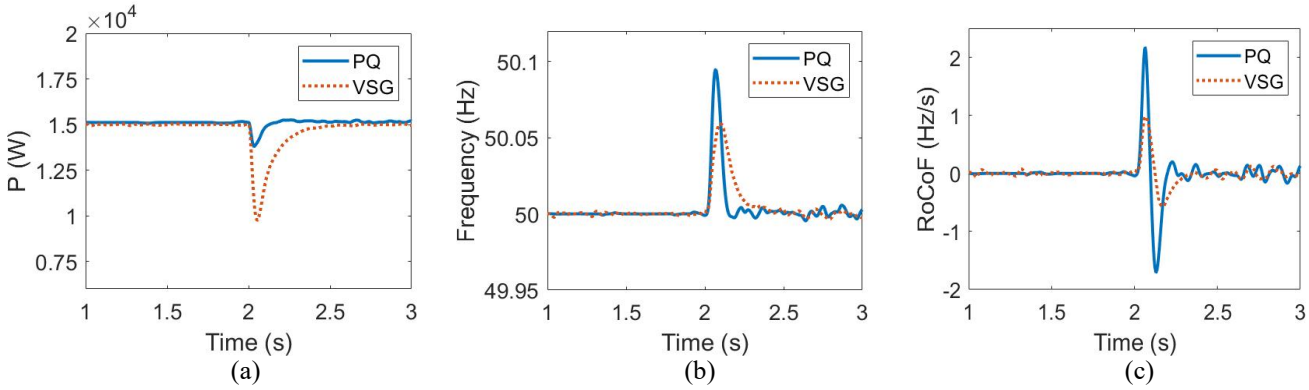

Fig. 8. Simulation waveforms under a load shed. (a) Inverter output power; (b) Frequency at the PCC; (c) RoCoF at the PCC.

C. *Under different SCR*

The SCR is used to measure the strength of the power grid and can be expressed as [16]:

$$SCR = \frac{P_{sc}}{P_{DCrated}} = \frac{V_g^2}{Z_g P_{DCrated}} \tag{3}$$

where P_{SC} is the short circuit power of the power grid; $P_{DCrated}$ is the power of the installed generator; V_g is the grid voltage; Z_g is the impedance of the grid. It is noted that the SCR can be changed through changing the value of Z_g. Long transmission lines and large grid impedance lead to the low SCR value. The higher the SCR value is, the stronger the power grid is. When 2<SCR<3, the power grid is weak and when SCR<2, the power grid is very weak [17].

The simulation waveforms of frequency and RoCoF at the PCC under different SCR are shown in Fig. 9 and Fig. 10, respectively. During 2~3s, a load step of 12 kW is applied to the power grid. As shown in Fig. 9 and Fig. 10, the load step has a larger influence on the power grid when the value of SCR is small. Furthermore, the VSG control can increase the frequency nadir and decrease the RoCoF to reduce the impact and improve the stability of the power grid. When SCR=1, the GFL converter cannot contain the stable operation during the load step, while GFM converter still stays stable. Although the maximum value of RoCoF exceeds the limits of IEEE 1547-2018 standard, it can be solved by regulating the value of virtual inertia and damping coefficient.

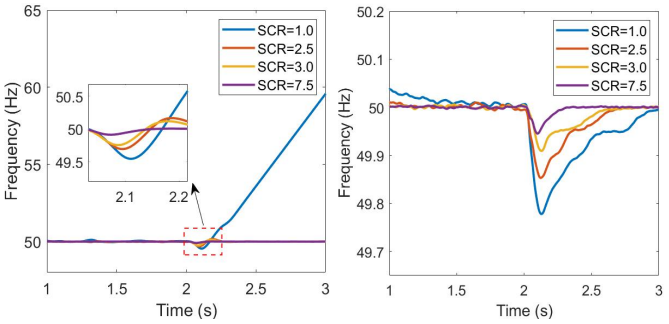

Fig. 9. Simulation waveforms of frequency at the PCC under different SCR. (a) PQ control; (b) VSG control.

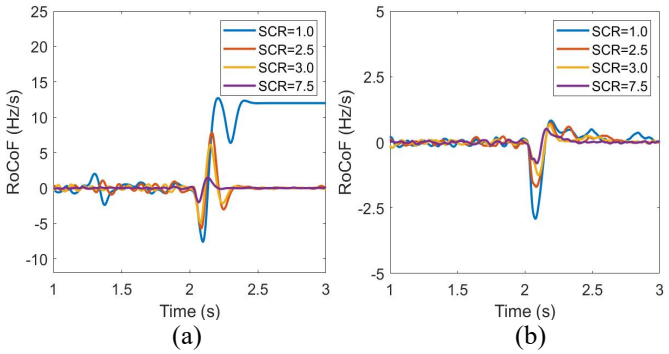

Fig. 10. Simulation waveforms of RoCoF at the PCC under different SCR. (a) PQ control; (b) VSG control.

VI. CONCLUSION

This paper analyzed the control structure of GFL control and GFM control. A case study was exemplified to compare the performance of GFL control and GFM control under different working conditions. It was demonstrated that the grid-connected converter with the GFM control is able to slow down the change of power and frequency, which reflects the inertial response characteristics like synchronous generator and improves the ability of power grid to cope with the sudden frequency disturbances, i.e., loss of generation and load fluctuations. Through the analysis of the simulation results, it was also revealed that the smaller the SCR becomes, the larger influence the load step has on the power grid. In addition, the GFM converter is more suitable for the weak power grid with low inertia.

References

[1] J. Fang, H. Li, Y. Tang, and F. Blaabjerg, "Distributed Power System Virtual Inertia Implemented by Grid-Connected Power Converters," *IEEE Trans. on Power Electronics,* vol. 33, no. 10, pp. 8488-8499, Oct. 2018.

[2] Q. Peng, Q. Jiang, Y. Yang, T. Liu, H. Wang, and F. Blaabjerg, "On the Stability of Power Electronics-Dominated Systems: Challenges and Potential Solutions," *IEEE Trans. on Industry Applications,* vol. 55, no. 6, pp. 7657-7670, Nov.-Dec. 2019.

[3] R. H. Lasseter, Z. Chen, and D. Pattabiraman, "Grid-Forming Inverters: A Critical Asset for the Power Grid," *IEEE Journal of Emerging and Selected Topics in Power Electronics,* vol. 8, no. 2, pp. 925-935, Jun. 2020.

[4] J. Rocabert, A. Luna, F. Blaabjerg, and P. Rodríguez, "Control of Power Converters in AC Microgrids," *IEEE Trans. on Power Electronics,* vol. 27, no. 11, pp. 4734-4749, Nov. 2012.

[5] M. Chen, D. Zhou, and F. Blaabjerg, "Modelling, Implementation, and Assessment of Virtual Synchronous Generator in Power Systems," *Journal of Modern Power Systems and Clean Energy,* vol. 8, no. 3, pp. 399-411, May 2020.

[6] X. Wang, M. G. Taul, H. Wu, Y. Liao, F. Blaabjerg, and L. Harnefors, "Grid-Synchronization Stability of Converter-Based Resources—An Overview," *IEEE Open Journal of Industry Applications,* vol. 1, pp. 115-134, 2020.

[7] W. Du, F. Tuffner, K. P. Schneider, R. H. Lasseter, J. Xie, Z. Chen, and B. P. Bhattarai, "Modeling of Grid-Forming and Grid-Following Inverters for Dynamic Simulation of Large-Scale Distribution Systems," *IEEE Trans. on Power Delivery,* 2020, early access, doi: 10.1109/TPWRD.2020.3018647.

[8] R. Rosso, X. Wang, M. Liserre, X. Lu, and S. Engelken, "Grid-Forming Converters: Control Approaches, Grid-Synchronization, and Future Trends—A Review," *IEEE Open Journal of Industry Applications,* vol. 2, pp. 93-109, 2021.

[9] D. Pattabiraman, R. H. Lasseter, and T. M. Jahns, "Comparison of Grid Following and Grid Forming Control for a High Inverter Penetration Power System," *in Proc. of PESGM 2018*, pp. 1-5, 2018.

[10] A. Sangwongwanich, A. Abdelhakim, Y. Yang, and K. Zhou, "Control of Single-Phase and Three-Phase DC/AC Converters," *Control of Power Electronic Converters and Systems*. Academic Press, 2018, pp. 153-173.

[11] A. K. Adapa, and V. John, "Virtual resistor based active damping of LC filter in standalone voltage source inverter," *in Proc. of APEC 2018*, pp. 1834-1840, 2018.

[12] Q. Zhong, and G. Weiss, "Synchronverters: Inverters That Mimic Synchronous Generators," *IEEE Trans. on Industrial Electronics,* vol. 58, no. 4, pp. 1259-1267, Apr. 2011.

[13] Q. Peng, Y. Yang, T. Liu, and F. Blaabjerg, "Coordination of Virtual Inertia Control and Frequency Damping in PV Systems for Optimal Frequency Support," *CPSS Transactions on Power Electronics and Applications,* vol. 5, no. 4, pp. 305-316, Dec. 2020.

[14] W. Wu, L. Zhou, Y. Chen, A. Luo, Y. Dong, X. Zhou, Q. Xu, L. Yang, and J. M. Guerrero, "Sequence-Impedance-Based Stability Comparison Between VSGs and Traditional Grid-Connected Inverters," *IEEE Trans. on Power Electronics,* vol. 34, no. 1, pp. 46-52, 2019.

[15] *IEEE Standard for Interconnection and Interoperability of Distributed Energy Resources with Associated Electric Power Systems Interfaces*, Standard 1547-2018, IEEE, New York, NY, USA, Apr. 2018.

[16] Q. Liu, T. Caldognetto, and S. Buso, "Stability Analysis and Auto-Tuning of Interlinking Converters Connected to Weak Grids," *IEEE Trans. on Power Electronics,* vol. 34, no. 10, pp. 9435-9446, Oct. 2019.

[17] A. A. A. Radwan, and Y. A. I. Mohamed, "Improved Vector Control Strategy for Current-Source Converters Connected to Very Weak Grids," *IEEE Trans. on Power Systems,* vol. 31, no. 4, pp. 3238-3248, 2016.